

ate and calcium sulfate, on the basis of analyses of contiguous sediment samples. Depth and surface area were recalculated for each step with morphometric data for the basin. The initial lake elevation before the rise during the glacial maximum was 1852 m, on the basis of shoreline gravels linked to basin-center stratigraphy. Before the rise in elevation, TDS was set to 8000 mg liter⁻¹, which is somewhat lower than previously estimated for this unit by F. W. Bachhuber [*Geol. Soc. Am. Bull.* **101**, 1543 (1989)]. This lower TDS value was chosen as a conservative estimate of runoff and corresponds to the upper part of the optimal range for *C. rawsoni* [D. R. Engstrom and S. R. Nelson, *Palaeontol. Palaeolimnol. Palaeoceanogr.* **83**, 295 (1991)], which is present in small numbers in this interval. The TDS in

runoff from snowmelt and streamflow was set to 100 mg liter⁻¹, about half the concentration in five modern spring-fed streams in the upland drainage. In ground water, TDS was set to 2100 mg liter⁻¹, on the basis of an average of five water wells nearest the zone of ground-water discharge. The ground-water discharge rate was set to 1.25×10^9 m³ year⁻¹. This value was reached on the basis of the average rate of accumulation of calcium carbonate and calcium sulfate in the lake bed and on the assumption that there is a long-term balance between the input of dissolved solids in ground water and their removal to sediments. This value is on the same order of magnitude as an estimate of ground-water discharge for the modern hydrologic system by B. E. DeBrine [thesis, New Mexico

Institute of Mining and Technology (1971)].
 8. L. B. Leopold, *Am. J. Sci.* **219**, 152 (1951).
 9. E. Antevs, *J. Geol.* **62**, 182 (1954).
 10. J. E. Kutzbach and H. E. Wright, *Quat. Sci. Rev.* **4**, 147 (1985).
 11. S. Hosteller and L. E. Benson, *Clim. Dyn.* **4**, 207 (1990).
 12. W. S. Broecker and G. H. Denton, *Geochim. Cosmochim. Acta* **53**, 2465 (1989).
 13. P. M. Grootes and M. Stuiver, *Eos* **73**, 258 (1992).
 14. We thank F. W. Bachhuber for providing several radiocarbon dates and L. V. Benson and P. De Deckker for comments. Supported by National Science Foundation grant EAR-9019134.

21 December 1992; accepted 23 March 1993

Spatiotemporal Patterns in the Energy Release of Great Earthquakes

Barbara Romanowicz

For the past 80 years, the energy released in great strike-slip and thrust earthquakes has occurred in alternating cycles of 20 to 30 years. This pattern suggests that a global transfer mechanism from poloidal to toroidal components of tectonic plate motions is operating on time scales of several decades. The increase in seismic activity in California in recent years may be related to an acceleration of global strike-slip moment release, as regions of shear deformation mature after being reached by stresses that have propagated away from regions of great subduction decoupling earthquakes in the 1960s.

The contributions of toroidal and poloidal components of global tectonic plate motions are about equal (1). The poloidal component, associated with upwelling and downwelling currents, is directly related to density variations in the deep mantle. The toroidal component, which represents horizontal shearing, exists primarily because of the presence of the rigid lithospheric plates and the associated heterogeneity in rheology. In addition to aseismic motions, which are difficult to observe, the poloidal component is expressed in thrust and normal faulting and the toroidal one, in strike-slip earthquakes. Yet the temporal pattern of seismic energy release is dominated by that of great thrust earthquakes, which are more than one order of magnitude larger than the largest strike-slip earthquakes. The contribution of the latter has therefore largely been ignored in analyses of temporal patterns of global seismic moment release.

In this report, I examine the spatiotemporal distribution of great shallow earthquakes since 1920 by taking into account the fault geometry and, as a first approximation, by considering two classes of earthquakes separately: strike-slip and subduction zone thrust earthquakes. Data are taken from the CMT (Centroid Moment Tensor) catalog (2) for the past 15 years, as well as from catalogs of great earthquakes in the

last century (3, 4) and a recently published catalog of large earthquakes by Pacheco and Sykes (PS) (5).

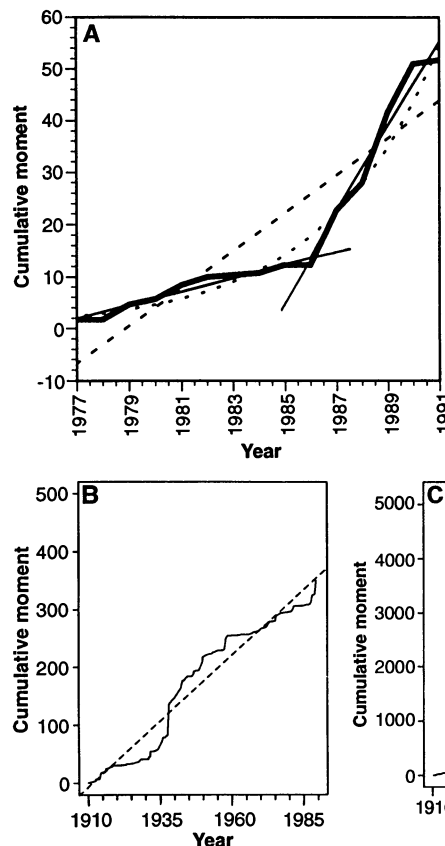


Fig. 1. (A) Cumulative moment released by strike-slip earthquakes in the past 15 years, from the CMT catalog (2). In all figure parts, the units of cumulative moment are 10^{20} N-m. The calculation is done with a yearly increment. All strike-slip earthquakes of moment larger than 0.1×10^{20} N-m have been included, where strike-slip is defined as corresponding to a mechanism with minimum dip of both nodal planes of 55° . The results are robust with respect to changes by 5° to 10° in this definition. For reference, the best fitting linear curve (dashed line) and the best fitting exponential curve (dotted line), where $\Sigma M = M_0 e^{+t/\tau}$, are shown; the rise time τ for the exponential fit is about 5 years. If we remove the Macquarie Island earthquake of 23 May 1989 from consideration, the rise time remains ~ 5 years. Also shown are separate linear fits for the periods 1977 to 1986.

(B) Cumulative moment release by strike-slip earthquakes in the PS catalog (5). (C) Same as (B) for non-strike-slip earthquakes. Note the change of scale from (B) to (C). Most of the great strike-slip earthquakes would disappear into the background if both types of earthquakes were plotted together.

Seismographic Station and Department of Geology and Geophysics, University of California, Berkeley, CA 94720.

release by earthquakes has decreased significantly in the past 20 years (5).

Great earthquakes, as defined by their magnitude or seismic moment, are dominated by subduction zone decoupling events. A more physical definition, from the point of view of plate tectonics, is to consider all decoupling earthquakes, that is, those that rupture the brittle zone in its entire thickness. For strike-slip earthquakes, the saturation of the downdip width of the fault occurs when it is commensurable with the thickness of the brittle zone (~10 to 25 km). The corresponding change of scaling observed for this type of earthquake is for moments of 0.6×10^{20} to 1.0×10^{20} N-m (12). For subduction zone events, on the global scale, such a limit is more difficult to define, in that saturation widths vary from region to region (from 50 km to more than 250 km) (13). On average, however, the downdip width of a decoupling earthquake will be at least five to ten times that for a strike-slip event. The temporal pattern of moment release (MR) during the last century is dominated by events of moment $M_0 > 20 \times 10^{20}$ to 50×10^{20} N-m (thrust) and 3×10^{20} to 5×10^{20} N-m (strike-slip). I therefore adopt this

definition for great events (listed in Table 1). For thrust events, this definition is more restrictive than in earlier studies (3).

The accuracy of moment estimates, especially for historical earthquakes, has been the subject of debate (3, 5, 14). Even for the recent largest earthquakes, a discrepancy in moment of a factor of 2 between different studies is not uncommon (5). This is, as discussed below, not a serious problem in my analysis. For earthquakes before the 1950s, moment has often not been measured directly but rather has been inferred from the reported magnitude. As for mechanisms, they have been assigned on the basis of indications given in the catalogs. A number of large earthquakes, primarily be-

fore the 1940s, have uncertain mechanisms. I arbitrarily assigned mechanisms to them, according to the prevailing mechanisms in the region in which they occurred and the current plate tectonic configuration. More accurate estimates of moment and mechanism are available for the past 20 years. For this reason, I initially analyzed the CMT catalog, complementing it thereafter with the PS catalog.

The cumulative MR by strike-slip earthquakes in the past 15 years, as obtained from the CMT catalog, shows an acceleration in MR since 1987 (Fig. 1A). This is due to the contribution of eight strike-slip earthquakes of moment larger than 1×10^{20} N-m that occurred between 1987 and

Table 1. Great earthquakes in the time period from 1920 to 1991. Moments are from (5); when several determinations are available, they are indicated. Listed are earthquakes of moment greater than 3×10^{20} N-m with strike-slip and uncertain mechanisms and earthquakes of moment greater than 20×10^{20} N-m with thrust or normal mechanism; FZ, fault zone.

Date	Moment (10^{20} N-m)	Region	Type of mechanism
11/11/1922	69.0, 140.0	Chile	Thrust
03/02/1923	70.0, 44.0, 200.0	Kamchatka	Thrust
26/06/1924	30.0	Macquarie	Unknown
03/09/1928	4.1	Ninety East Ridge	Strike-slip
27/06/1929	12.0	South Sandwich	Unknown
10/08/1931	8.5, 24.9	Altai	Strike-slip
02/03/1933	40.0	Japan	Normal
20/09/1935	14.5	New Guinea	Uncertain (strike-slip)
28/12/1935	5.9	Sumatra	Strike-slip
01/02/1938	52.0, 70.0, 27.2	Banda Sea	Strike-slip
10/11/1938	28.5, 12.3	Alaska	Thrust
25/01/1939	3.5	Central Chile	Uncertain (strike-slip)
26/12/1939	3.5	Anatolian Fault	Strike-slip
25/11/1941	15.7	Azores	Strike-slip
10/11/1942	13.0, 44.5	Prince Edward FZ	Strike-slip
06/04/1943	25.0, 28.0	Chile	Thrust
12/09/1946	3.5	Burma	Uncertain (strike-slip)
24/06/1948	14.0	Philippines	Unknown
22/08/1949	13.0	Queen Charlotte I.	Strike-slip
17/12/1949	4.9	North Scotia	Strike-slip
17/12/1949	4.9	North Scotia	Strike-slip
15/08/1950	95.0	Tibet	Thrust
18/11/1951	4.6	Tibet	Strike-slip
04/11/1952	350.0	Kamchatka	Thrust
04/12/1957	18.0, 13.0	Altai	Strike-slip
09/03/1957	585, 400	Aleutians	Thrust
10/07/1958	5.3, 4.4	Queen Charlotte I.	Strike-slip
06/11/1958	44.0, 40.0	Kuriles	Thrust
22/05/1960	1900, 1600	South Chile	Thrust
13/10/1963	67, 50, 75	Kuriles	Thrust
28/03/1964	750.0	Alaska	Thrust
24/01/1965	13.0, 24.0	Banda Sea	Thrust
04/02/1965	48, 140	Aleutians	Thrust
16/05/1968	28.0	Japan	Thrust
11/08/1969	22.0	Kuriles	Thrust
30/07/1972	3.0	Queen Charlotte I.	Strike-slip
26/05/1975	7.0	Azores	Strike-slip
04/02/1976	3.7, 2.6	Guatemala	Strike-slip
19/08/1977	30.0	Sumbawa	Normal
12/12/1979	29.0	Columbia	Thrust
25/05/1981	5.0	Macquarie	Strike-slip
20/10/1986	4.5	Kermadec	Strike-slip
30/11/1987	7.3	Alaska	Strike-slip
23/05/1989	13.6	Macquarie	Strike-slip
03/03/1990	3.0	Fiji	Strike-slip
16/07/1990	4.1	Philippines	Strike-slip

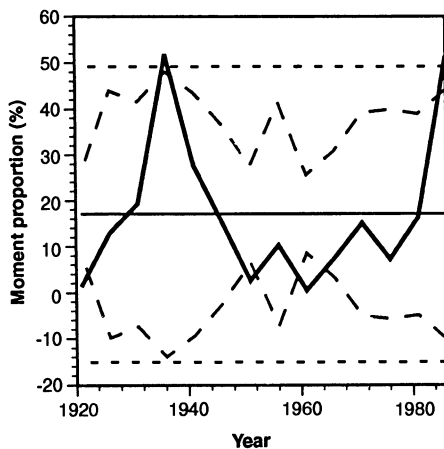


Fig. 2. Proportion of moment released in strike-slip earthquakes as compared to total moment release, calculated in 5-year bins for earthquakes of moment greater than 0.1×10^{20} N-m in the period from 1920 to 1990. The solid horizontal line is the average moment proportion for that period, and straight dashed lines are 95% confidence limits calculated for the entire period. Jagged broken lines are 95% confidence limits calculated on the basis of a test of the null hypothesis that the yearly moment proportions are uncorrelated in each 5-year period. Both peaks in 1935 to 1940 and 1985 to 1990 are significant. All observed peaks are the results of contributions from more than one great earthquake. The periods of lowest moment proportion in 1950 to 1955 and 1960 to 1965 are also significant for the second test (long dashed lines). This statistical argument is limited because quoted moments have unknown uncertainties, which may be large.

1991, compared to only three in the previous 10 years. The strongest contribution in this 5-year period is from the Macquarie Ridge earthquake of 23 May 1989, which is also the largest earthquake (regardless of mechanism) in the last 12 years. This earthquake alone is not the cause for the observed pattern: the total MR in the 5-year period from 1987 to 1991 is about five times that in the preceding two 5-year periods; it is still three times larger if the Macquarie Ridge event is omitted. Also, the MR in each of the 4 years from 1987 to 1990 is more than 2 SD larger than the average per year in the preceding 10 years.

The cumulative moment for strike-slip earthquakes from 1900 to 1989, from the PS

catalog (Fig. 1B), confirms the trend already noted for the time period from 1977 to 1991 based on the CMT catalog, the rate of MR being low from 1960 to 1986. Two earlier periods of accelerated MR are evident, one around 1940 and the other at the beginning of the century. The former is due to six strike-slip events of moment greater than 5×10^{20} N-m that occurred from 1931 to 1942, whereas none occurred from 1907 to 1923 and none from 1960 to 1974. The acceleration in 1905, dominated by the Altai events of July 1905, may have been largely overestimated. I conclude that episodes of large and small MR in strike-slip earthquakes have alternated worldwide, at least in the last 80 years.

The cumulative MR by non-strike-slip

earthquakes, as given in the PS catalog (Fig. 1C), shows one clear period of accelerated MR around 1960. This period is well documented (3, 11) and is due primarily to five subduction zone decoupling events, each of $M_0 > 100 \times 10^{20}$ N-m (Table 1). This period falls largely between periods during which strike-slip activity was enhanced.

A plot (Fig. 2) of the ratio of MR in strike-slip earthquakes with respect to the total MR, for the period from 1920 to 1991, further illustrates the alternation of MR in great strike-slip and thrust events. The two main periods of accelerated MR in strike-slip earthquakes are also periods in which this ratio increased by a factor of 2 or more. Although the two great normal faulting events (Table 1) were included in this comparison, the observations remain robust if these events are removed.

The geographical distribution of MR, for four consecutive 20-year periods of strike-slip (Fig. 3, A to D) and thrust events (Fig. 3, E to H), reveals several patterns. The concentration of great thrust events from 1950 to 1970 primarily covers the Pacific plate boundary between Japan and Alaska. Since 1970, the occurrence of large strike-slip earthquakes may represent a continuation of Mogi's (11) progression pattern along the Pacific plate boundary, toward the northeast and the southwest, to cover the remaining nonspreading parts of this boundary. This pattern is indicative of a process of stress transfer along adjacent plate boundaries with a rate of several thousand kilometers in 10 to 20 years, in good agreement with the concept of accelerated plate tectonics (15, 16) in which stresses can be transferred over large distances in an elastic lithosphere underlain by a viscous asthenosphere.

The second trend evident in Fig. 3 is the occurrence, during periods of accelerated strike-slip MR, of great earthquakes at locations far removed from the western Pacific plate boundaries, such as in the Azores and the south Indian Ocean. These patterns are suggestive of a global coupling phenomenon involving stress transfer from poloidal to toroidal motion. The transfer would have to be rapid and followed by a period of maturing in regions of toroidal energy release. Whether the excitation mechanism is internal (ridge push, slab pull) or external [for example, Earth's rotation (3, 8)] and whether it has any periodicity remain to be determined, but the observed time scale of the process, associated with increased accuracy in the quantification of earthquakes, raises the hope that improved understanding could be gained in the next 20 years.

The alternation, during the past 80 years, in MR between strike-slip earthquakes and great subduction zone earthquakes readily

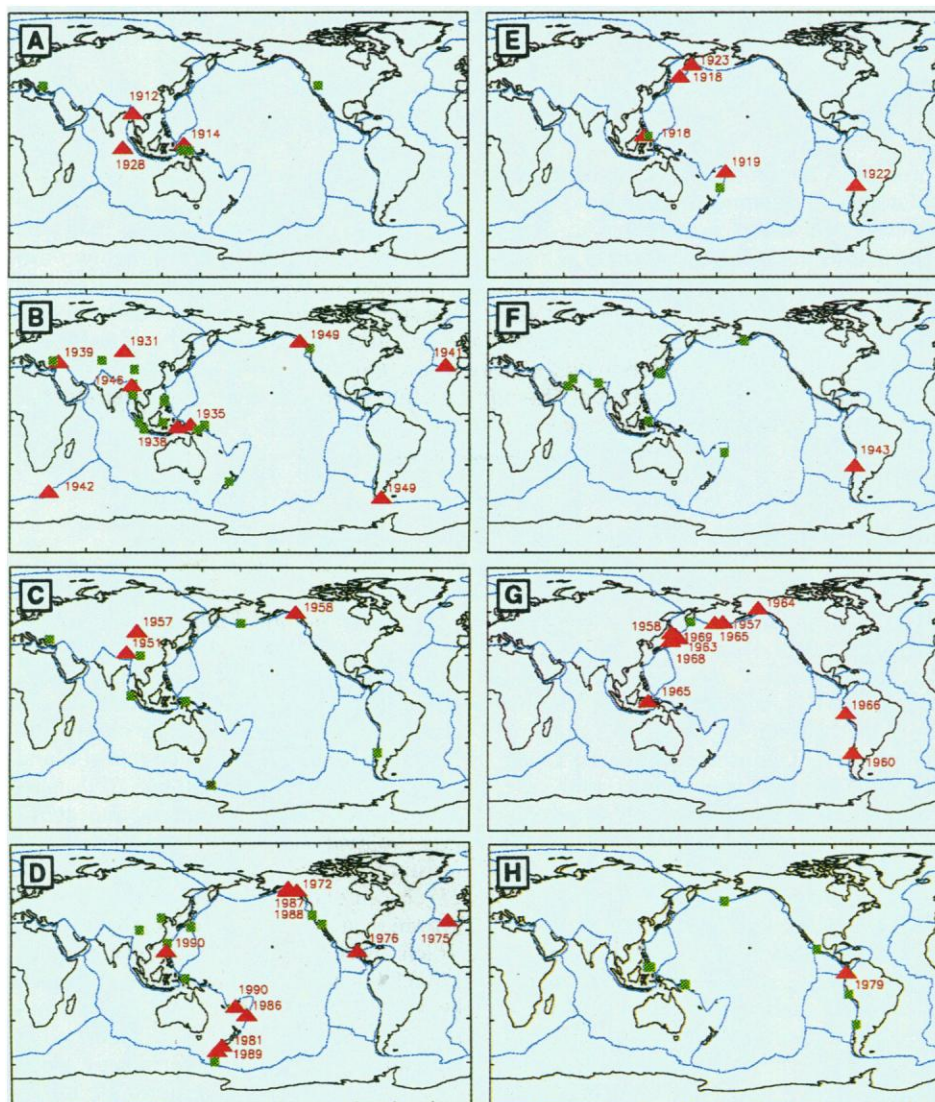


Fig. 3. Space-time distribution of large and great earthquakes in the period 1908 to 1991. Strike-slip earthquakes: (A) 1908 to 1928, (B) 1929 to 1949, (C) 1950 to 1970, and (D) 1971 to 1992. Thrust earthquakes: (E) 1908 to 1928, (F) 1929 to 1949, (G) 1950 to 1970, and (H) 1971 to 1992. For (A) to (D) squares are for strike-slip earthquakes with moment greater than 1×10^{20} N-m, triangles and years of occurrence are for those with moment greater than 3×10^{20} N-m. For (E) to (H) squares are for thrust earthquakes with moment greater than 5×10^{20} N-m and less than 20×10^{20} N-m; triangles and years of occurrence are for those with moment greater than 20×10^{20} N-m. The maps for the earliest periods (A and E) are relatively uncertain and are given only for reference.

explains the decrease in total MR in the past 20 years, in which strike-slip events have been active, producing moments that are smaller (1/10 to 1/20) than those in periods of accelerated subduction zone activity. The large contribution of aseismic energy release in strike-slip systems provides an explanation for the discrepancy in MR for the two types of earthquakes. Mogi (17) proposed that different parts of plate boundaries go through alternating periods of high and low activity, on a time scale of tens of years. This notion and the patterns revealed in the earthquake catalogs imply that the increase in seismic activity at large magnitudes ($M > 5$) in California since 1985 (18) or along the Anatolian fault in the 1940s (19) may be regional manifestations of a larger scale phenomenon involving stress transfer from subduction zones to zones of toroidal energy release and resulting in activation of specific parts of plate boundaries.

Although the large-scale progressions of great earthquakes around the Pacific and the Nazca plate have been noted, the implications have not been incorporated explicitly in the identification of seismic potentials of gaps (20). If the notion that portions of plate boundaries are activated in a nonrandom manner on time scales of tens of years and geographical scales of several thousands of kilometers is valid, it might be used to more accurately predict the time of occurrence of great earthquakes. The seismic gap theory has recently been challenged on the basis of statistical analysis of event occurrence in the past 20 years, primarily in subduction zone areas (21). According to my study, the resolution of this question may have to wait until the next period of increased activity in great subduction zone decoupled earthquakes.

This study may provide the basis for more quantitative testing of several hypotheses concerning the stress transfer from the underlying convective mantle to the tectonic plates. Data accumulated over another 10 or 20 years may be sufficient to sort out the causal relationships involving the Earth's rotation, internal processes, and earthquake energy release. In particular, we may be able to monitor deformation related to plate tectonics, not only as averaged over geological time scales but over several decades—the scale of the Global Change Program. More precise knowledge of moments and mechanisms of great earthquakes at the turn of the century would also be very valuable, if only to shed light on the possible periodicity in the alternation of great strike-slip and thrust earthquakes.

REFERENCES AND NOTES

1. R. O'Connell, C. Gable, B. Hager, *Glacial Isostasy, Sea Level, and Mantle Rheology* (Kluwer Academic, Dordrecht, Netherlands, 1990).

2. A. M. Dziewonski, G. Ekstrom, J. Woodhouse, G. Zwart, *Phys. Earth Planet. Inter.* **62**, 194 (1990).
3. H. Kanamori, *J. Geophys. Res.* **82**, 2981 (1977).
4. K. Abe, *J. Phys. Earth* **23**, 381 (1975).
5. J. F. Pacheco and L. R. Sykes, *Bull. Seismol. Soc. Am.* **82**, 1306 (1992).
6. J. Brune, *J. Geophys. Res.* **73**, 777 (1968).
7. F. A. Dahlen, *Geophys. J. R. Astron. Soc.* **32**, 203 (1973).
8. D. L. Anderson, *Science* **186**, 49 (1974).
9. R. J. O'Connell and A. M. Dziewonski, *Nature* **262**, 259 (1976).
10. A. Souriau and A. Cazenave, *Earth Planet. Sci. Lett.* **75**, 410 (1985).
11. K. Mogi, *J. Phys. Earth* **16**, 30 (1968).
12. B. Romanowicz, *Geophys. Res. Lett.* **19**, 481 (1992).
13. J. Kelleher, J. Savino, H. Rowlett, W. McCann, *J. Geophys. Res.* **79**, 4889 (1974).
14. G. Ekstrom and A. M. Dziewonski, *Nature* **332**, 319 (1988).
15. M. H. P. Bott and D. S. Dean, *ibid.* **243**, 339 (1973).
16. D. L. Anderson, *Science* **187**, 1077 (1975).
17. K. Mogi, *Tectonophysics* **22**, 265 (1974).
18. L. R. Sykes and S. C. Jaume, *Nature* **348**, 595 (1990).
19. M. N. Toksoz, A. F. Shakal, A. J. Michael, *Pure Appl. Geophys.* **117**, 1258 (1974).
20. J. Kelleher, L. R. Sykes, J. Oliver, *J. Geophys. Res.* **78**, 2547 (1973).
21. Y. Y. Kagan and D. D. Jackson, *ibid.* **96**, 21419 (1991).
22. I thank A. Dziewonski and C. Marone for discussions and encouragement and J. F. Pacheco for providing his catalog in digital form. D. Brillinger assisted with the statistical analysis.

19 January 1993; accepted 22 April 1993

Arabidopsis thaliana DNA Methylation Mutants

Aurawan Vongs,* Tetsuji Kakutani,† Robert A. Martienssen, Eric J. Richards†‡

Three DNA hypomethylation mutants of the flowering plant *Arabidopsis thaliana* were isolated by screening mutagenized populations for plants containing centromeric repetitive DNA arrays susceptible to digestion by a restriction endonuclease that was sensitive to methylated cytosines. The mutations are recessive, and at least two are alleles of a single locus, designated *DDM1* (for decrease in DNA methylation). Amounts of 5-methylcytosine were reduced over 70 percent in *ddm1* mutants. Despite this reduction in DNA methylation levels, *ddm1* mutants developed normally and exhibited no striking morphological phenotypes. However, the *ddm1* mutations are associated with a segregation distortion phenotype. The *ddm1* mutations were used to demonstrate that *de novo* DNA methylation *in vivo* is slow.

DNA methylation has been implicated in the control of a number of cellular processes in eukaryotes, including transcription (1), imprinting (2), transposition (3), DNA repair (4), chromatin organization (5, 6), and a variety of epigenetic phenomena (7), although the function of DNA methylation in eukaryotes remains the subject of continued debate. Using DNA methylation mutants to study the functions of DNA modification in eukaryotes is an attractive approach that avoids some of the limitations associated with correlative and methylation inhibitor studies. Li *et al.* (8) recently reported that mouse DNA methyltransferase mutants, generated by gene disruption, are unable to complete embryogenesis, although homozygous mutant cell lines are viable and apparently normal. We report here the isolation and characterization of DNA methylation mutants in the flowering

plant *Arabidopsis thaliana*.

We identified *A. thaliana* DNA methylation mutants by screening directly for plants that contained hypomethylated genomic DNA using Southern (DNA) blot analysis. Filters containing Hpa II–digested genomic DNA prepared from leaves of mutagenized *A. thaliana* plants were hybridized with a cloned 180-bp repeat found in long tandem arrays at all five *A. thaliana* centromeres (9). Centromeric repeat arrays isolated from wild-type plants are resistant to Hpa II (CCGG) digestion (10, 11) because of extensive methylation of cytosines at the CpG and CpNpG sites, which is characteristic of plants (12) [^{5m}CCGG and C^{5m}CGG are not digested by Hpa II (13)]. DNA methylation mutants, on the other hand, were predicted to contain hypomethylated centromeric arrays susceptible to Hpa II digestion. We examined Southern filters containing DNA from 79 pools representing approximately 2000 plants from ethyl methanesulfonate–mutagenized M₂ populations (ecotype Columbia) to look for centromere repeat multimers of low molecular weight that were clipped from the long arrays by Hpa II. Individual plants from candidate pools were

Cold Spring Harbor Laboratory, Cold Spring Harbor, NY 11724.

*Present address: Merck Research Laboratory, Rahway, NJ 07065.

†Present address: Department of Biology, Washington University, St. Louis, MO 63130.

‡To whom correspondence should be addressed.